REPORT DOCUMENTATION PAGE

Form Approved
OMB No. 0704-0188

1. REPORT DATE *(DD-MM-YYYY)*	2. REPORT TYPE	3. DATES COVERED *(From - To)*
30-04-2007	Final Report	Nov 2005 - Apr 2007

4. TITLE AND SUBTITLE
Ocean Wave Energy Harvesting Devices

5a. CONTRACT NUMBER
HR001-06-C-0030

5b. GRANT NUMBER

5c. PROGRAM ELEMENT NUMBER

6. AUTHOR(S)
Cheung, Jeffrey, T; Childress, Earl, F, III

5d. PROJECT NUMBER

5e. TASK NUMBER

5f. WORK UNIT NUMBER

7. PERFORMING ORGANIZATION NAME(S) AND ADDRESS(ES)

Teledyne Scientific &
Imaging, LLC
1049 Camino Dos Rios
Thousand Oaks, CA 91260

8. PERFORMING ORGANIZATION REPORT NUMBER

RC71273.FR

9. SPONSORING / MONITORING AGENCY NAME(S) AND ADDRESS(ES)

Defense Advanced Research Projects
Advanced Technology Office/ATO
3701 North Fairfax Drive
Arlington, VA 22203-1714

10. SPONSOR/MONITOR'S ACRONYM(S)
DARPA/CMO

11. SPONSOR/MONITOR'S REPORT NUMBER(S)
ARPA Order No. V233/00,Pgm Code 5X20

12. DISTRIBUTION / AVAILABILITY STATEMENT

Approved for public release; distribution unlimited.

13. SUPPLEMENTARY NOTES

The views and conclusions contained in this document are those of the authors and should not be interpreted as representing the official policies, either expressly or implied, of the Defense Advance Research Projects Agency or the U.S. Government.

14. ABSTRACT

Development of an ocean wave energy-harvesting device that can be used as a renewable energy source for ocean monitoring systems. The core technology is a mass-spring based high efficiency, low frequency linear generator that was integrated to a spar buoy to form a robust unit. Its dynamic sensitivity is improved by the use of a near zero friction liquid bearing. Through extensive theoretical modeling and wave tank testing, we studied the effect of enhanced heave motion due to resonance with waves and applied it to improve the energy harvesting efficiency. We also developed a computer simulation model that can accurately predict the device performance driven by a single frequency, sinusoidal forcing function. Full-scale models were fabricated and field tested in non-random waves. Power output was measure from 1.6 W to more than 6 W, depending on the device size, oscillator characteristic and wave conditions. Finally, we carried out extensive studies to build and characterize several small underwater motion energy harvesters of different designs. A complete performance metrics was established.

15. SUBJECT TERMS

16. SECURITY CLASSIFICATION OF:			17. LIMITATION OF ABSTRACT	18. NUMBER OF PAGES	19a. NAME OF RESPONSIBLE PERSON
a. REPORT	b. ABSTRACT	c. THIS PAGE			Cheung, Jeffrey T.
Unclassified	Unclassifed	Unclassified	SAR	32	19b. TELEPHONE NUMBER *(include area code)* 805 373-4144

Standard Form 298 (Rev. 8-98)
Prescribed by ANSI Std. Z39.18

TELEDYNE
SCIENTIFIC & IMAGING, LLC
A Teledyne Technologies Company

April 2007 **SC71273**

Ocean Wave Energy Harvesting Devices

Final Report

For 11/15/05 through 04/30/07

Contract No. HR0011-06-C-0030

Sponsored by
Defense Advanced Research Projects Agency
Advanced Technology Office/(ATO)
Program: Ocean Wave Energy Harvesting Devices
ARPA Order No. V233/00, Program Code: 5X20
Issued by DARPA/CMO under Contract No. HR0011-06-C-0030

J.T. Cheung
Program Manager

Summary

The goal of the Phase 2 program entitled "Ocean Wave Energy Harvesting Devices" was to develop a simple and robust wave energy-harvesting device that can be used as a renewable energy source for ocean monitoring systems. The technology is based on the well-known principle of passing a magnet through a coil to produce electrical power. However, this concept would be unfeasible without the near-zero-friction liquid bearings developed by Teledyne Scientific Company (TSC). This unique technology, combined with a low frequency linear generator, enables seamless integration with a tuned spar buoy to convert the mechanical energy of the wave motion into electricity. The device package is completely sealed from the marine environment and corrosion free. Based on the groundwork established in Phase 1 and extensive computer simulation and bench tests, we have further improved the generator and energy coupling mechanism to make it more robust with higher power output. Consequently, we have shown devices with power output from 1.6 Watts to over 6 Watts under different, albeit not well-characterized, wave conditions.

The Phase 2 program consisted of three major tasks. Task 1 and 2 required the development of wave energy harvesting devices to be operated in different sea states. These devices consist of a linear generator placed within a frequency-tuned spar buoy to take advantage of enhanced heave motion when the spar buoy natural period matches with the wave period at the deployment site. Energy from the heave motion can be transferred to the linear generator efficiently via resonance coupling. Single spar buoy devices were fabricated under Task 1 for operating in small waves with 2 and 3 second periods. A "tetra-spar" buoy device was fabricated under Task 2 for operation in waves with periods less than 2 seconds. In Task 3, we studied the feasibility of a small device to be mounted on fish to harvest energy while the fish moves in water. Both the translational and rotary devices were tested and their performance was assessed over a wide range of device size and movements. Finally, a computer model was developed to simulate and predict the performance of spar buoy based devices. Model calculations were compared to bench test and the results were in excellent agreement. Although the computer model and bench test were based on excitation from a single frequency sinusoidal forcing function, basic guidelines for system design and a mathematical framework were derived. These elements will require further development to simulate the device performance in more realistic ocean conditions.

The project team consisted of three groups. Teledyne Scientific Company was the project lead and was specifically responsible for the linear generator development and overall system design. Oceanscience Group, a buoy manufacturer, was responsible for full-scale device fabrication and field tests. The University of Rhode Island (Prof. Malcolm Spaulding of the Dept. of Ocean Engineering) provided hydrodynamic modeling and wave tank testing of scaled down models.

Table 1 below summarizes key aspects of the program and final report contents, as requested in the contract.

Table 1. Summary of key aspects of the program and final report contents.

Task Objectives	1. Develop **vertical heave energy harvesting device**, model buoy hydrodynamics, fabricate prototype, and field test at Sea State below 3, with target performance of 6 Watts at Sea State 1, and 30 Watts at Sea State 5. 2. Develop **tetrahedral wave energy harvesting device**, field test in low Sea States, with target performance of 2 Watts in Sea State 1 and 1 Watt in Sea State 5. 3. Develop **underwater energy harvesting device**, fabricate two basic configurations and test in wave tank for optimization.
Technical Problems	1. **Robustness and long-term survivability:** Historically, many ocean wave technologies have failed due to complex designs which were vulnerable to salt water corrosion and mechanical failures. 2. **Compact size:** Most ocean wave energy harvesting devices are intended for large scale power generation. These designs are too large to be mounted on moderate size ocean buoys for persistent surveillance. 3. **Efficient energy coupling:** Coupling must occur over a broad range of wave conditions while also maintaining robustness and long-term survivability.
General Methodology	Laboratory experiments, numerical and physical model simulations, prototype fabrication, wave tank testing, and field trials.
Technical Results	1. Axial generators should be used for all systems which allow for a linear design. Axial generators are more easily produced and provide comparable power when compared with transversal generators. 2. Transversal generators can be employed for designs which require curvature, though they are difficult to produce and require spring performance which is not easily achieved. 3. Phosphor-bronze and beryllium-copper springs are acceptable solutions for devices tuned to high frequency waves with periods less than 2 seconds. 4. Elastomer springs are acceptable for devices tuned to lower frequency waves, although sagging can potentially become an issue over the life of the device. 5. Spar buoys with power generators tuned to low frequency wave period resonances present significant size and spring performance challenges, making them somewhat impractical.
Important Findings and Conclusions	1. Harvesting energy in the range of 1-50 Watts from ocean waves in moderate sea states is very promising using the TSC device designs. The nearly frictionless ferrofluid-based mass-spring power generator design is robust and efficient. The generator has the potential to generate tens of watts of power on a continuous basis when properly coupled to a suitable buoy platform. 2. The approach of designing a device which meets the requirements for mounting on dogfish and generating continuously 200 mW is not feasible.
Significant Hardware Development	1. Two wave energy harvesting devices including power generators and buoys tuned for 2.3 and 3.0 second wave periods. 2. One tetrahedral spar buoy with tuned power generator device.
Special Comments	None
Implications for Future Research	1. Improve power generator simulation model to include real-world wave, wind, current conditions. 2. Broaden the response of the wave energy device to reduce the dependence on site conditions. 3. Field test wave energy harvesting devices of different size and generation capability, and correlate the performance with real time 3-axis accelerometer data in known wave, wind, and current conditions.

Table of Contents

1.0 Background

The ocean is a tremendous source of energy in the form of random waves and currents. Harvesting energy from these motions has been a subject of interest for centuries. However, numerous attempts have been unsuccessful as the device failed to survive the severe and corrosive marine environment. Even today, no reliable and cost effective solution has yet been developed. In this program, Teledyne Scientific Company (TSC, formerly Rockwell Scientific Company) presents a unique solution to address these challenges. The concept was first validated in Phase 1 (2/11/2003 through 5/11/2004, Contract No. MDA972-03-C-0025-CLN0001AB), in which we carried out fundamental studies on the near-zero friction ferrofluid bearings, fabricated low frequency linear generators and integrated the generator to a floating platform to produce 0.37 Watts of power from light wave waves just off the coastline in La Jolla, California. In Phase 2 we improved the performance by developing a mass-spring type low frequency linear generator, enabled by a near-zero-friction liquid bearing to improve its dynamic sensitivity and robustness. When the generator is integrated with a spar buoy tuned to the same frequency, the two oscillators become closely coupled and energy can flow between them without an internal barrier. Wave energy contained near the fundamental frequency of the device can be coupled into the device to generate electricity. The hermetically sealed system is mechanically robust and will not corrode.

1.1 Tasks

The Phase 2 task objectives are to develop and produce three types of wave motion energy harvesting devices to be used as renewable energy sources for ocean surveillance applications. The specific tasks were:

Task 1: Vertical Heave Energy Harvester
Task 2: Tetrahedral Autonomous Buoys
Task 3: Underwater Energy Harvesters

In this report, general issues and design considerations for all tasks are discussed in Chapters 2 and 3. The devices fabricated in response to Tasks 1 and 2 are discussed in Chapters 4, 5, and 6, as similarities in design led to certain overlap in those tasks. The underwater device corresponding to Task 3, which proved to be the least desirable approach, is discussed in detail in Chapter 7.

1.2 Team

There are three members in the team:

1) Teledyne Scientific and Imaging Company (TSC)
Prime contractor: Linear generator design and fabrication; device design; computer simulation; bench and field test.

2) University of Rhode Island (URI)
Subcontractor: Hydrodynamic modeling and wave tank test

3) Subcontractor: Oceanscience Group (OS)
Buoy design/manufacturing and field test

1.3 Achievements

In Phase 2, we improved the wave energy harvester to make it more robust and efficient. Two basic designs were developed under Tasks 1 and Task 2. They share a similar linear generator and key features but use different buoy platforms. In Task 1, we developed single spar buoys tuned to natural periods of 2.3 sec and 3.0 sec and fitted them with linear generators tuned to the same frequencies. In Task 2, we developed a tetra-spar buoy based device to respond to smaller but faster (1.7 second) waves. The single buoy devices were field tested in highly regular boat wakes in a harbor. They produced over 6 Watts (2.3 second device) and 4 Watts (3.3 second device) of continuous power in approximately 10-inch high waves with nearly the same periods. These waves were uni-directional and narrowly-distributed frequencies. The test results therefore did not accurately reflect what would happen in random ocean waves.

Parallel to the device design, fabrication and field tests, we also developed a computer simulation model based on solving a set of coupled oscillator equations with damping terms. The model was validated by "dry" bench tests (simulated by a spring apparatus hanging from the lab ceiling) under controlled conditions. In this case, the model and the bench test were limited to excitation from a single frequency, in a sinusoidal waveform. Although this approximation does not approximate random ocean waves, the simulation model provided invaluable guidelines for the device design.

In Task 3, we carried out a systematic study to access the performance metrics of two types of small motion energy generators that could be used on the tail of a marine life such as dogfish to harvest energy as it swims. The output power can be used to trickle charge battery packs to power sensors mounted on the body. However, we discovered that this approach could not provide sufficient power to meet the goal given the size and weight constraints and the slow movement of the fish.

Finally, we discussed the advantages and disadvantages of spar buoy based wave energy harvesting device and pointed out its limitations. In addition, based on our studies we also conceived a few improved concepts to further advance this technology.

2.0 Technical hurdles

This program faced three principal technical hurdles

1) **Robustness and long-term survivability:** Historically, many ocean wave technologies have failed due to complex designs which were vulnerable to salt water corrosion and mechanical failures. To solve this problem, we need a simple design that is statically sealed.

2) **Compact size:** Most ocean wave energy harvesting devices are intended for large scale power generation. These designs are too large to for the requirements of the ocean surveillance systems. To solve this problem, we need a design that is compact and easily deployable either as a stand-alone unit or as an add-on unit to an existing system.

3) **Efficient energy coupling:** Conventional ocean energy harvesting technologies have adequately addressed this problem by using direct coupling mechanisms. But they were accomplished either by using an open system or through dynamic motion seals. Both approaches have lifetime issues in the sea. To solve this problem, we face the challenge to design a system that is statically sealed but capable of efficient energy coupling in a broad range of wave conditions.

In the following sections, we address these problems and provide solutions.

3.0 Wave energy harvesting device design

Most wave energy harvesting devices have two major components: a floating platform and an electrical generator. The floating platform should be designed to efficiently couple with the wave motion over a wide range of ocean conditions, so that the wave energy can be converted to electricity by the on-board generator. The electrical generator should have high conversion efficiency in low frequency operation in order to match with the wave motion. In addition, the conversion of motion energy to electricity must take place in a time much shorter than one wave period, so as not to be affected by the arrival of the subsequent waves. Most important of all, the device must be robust enough to survive the marine environment. Devices developed under this program were designed to target their performance toward these goals.

3.1 Linear generator design

The core component of a wave energy-harvesting device is the generator. It converts mechanical energy to electricity by moving an array of permanent magnets through a set of conductive coils. According to the Faraday principle, the induced voltage across the coil is given by:

$$V = NA\, d\Phi/dt$$

Where N is the number of turns in the coil, A is the average area enclosed by the coil, and Φ is the magnetic flux density normal to the area encircled by the coil. The amount of electrical energy, $E = V^2/R_L$, can be extracted by a resistive load R_L, such as a rechargeable battery and its associated circuit elements. Most generators have a rotary design that is compact and cost effective. However, these devices are designed to run at very high rotational speed. When they are used to harvest energy from the slower moving waves, they must be used in conjunction with a complex velocity up-converter. Some examples of velocity up converters are: hydraulics (Pelamis and Power Buoy), rack and pinion (latest model of Power Buoy) and gears (Salter Duck). Although these systems can produce many kilowatts of power, they are too cumbersome for the applications in this program. In addition, the velocity up conversion mechanisms are vulnerable to the harsh ocean environment. Our mass-spring type linear generator can alleviate this problem. In this design, the magnet stack is mounted on a spring and oscillates reciprocally through a set of induction coils to generate power. It allows the use of a heavy magnet stack with a special design to provide high magnetic flux density perpendicular to the coils to compensate for the lack of speed. Two linear generator designs were studied and tested: Axial Linear Generator and Transversal Linear Generator. Extensive magnetic analysis and experimental measurements were made for both designs in order to optimize the dimensions of the individual component. Their design, principle of operation, advantages, and disadvantages are discussed below.

3.2 Axial linear generator

By definition, in an axial linear generator, the magnetic flux to be captured by coils has the same direction as the movement of the magnetic stack. Fig.1 shows the schematic of this design. The magnetic stack consists of cylindrical permanent magnets stacked together with opposing polarity between the adjacent segments separated by a thin low carbon steel spacer. A thin low carbon steel cap also covers both ends of the stack. The magnet stack is connected to a spring to form a spring-mass system inside a tubular housing wrapped with bands of induction coils. NdFeB grade 42 rare earth magnets are used. This material has a high saturation field, cohesive energy and Curie temperature; therefore it can retain its magnetic properties for an infinite period of time. The spacer acts as a low magnetic reluctance path to combine the fluxes from adjacent magnets and direct them outward to loop around the coil and return to the next spacer. The magnetic field in the free space just outside of the edge of space is nearly 10,000 Gauss. A small amount of ferrofluid was applied to the magnet stack surface and immediately encircled the spacers to form rings of liquid cushions as shown in Fig. 2. These rings of near zero friction bearings facilitate the movement between the magnet stack and the tubular wall of the generator and completely prevent the magnet from making direct contact to the tube wall even when the device is inclined far from the vertical position. The fluid eliminates the frictional wear and increases the device dynamic sensitivity to capture energy from the slightest movements.

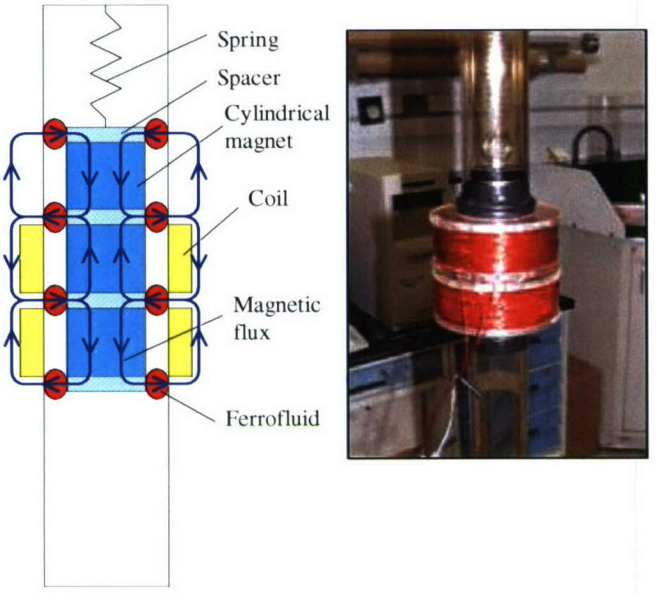

Fig. 1. Schematic of an axial linear generator.

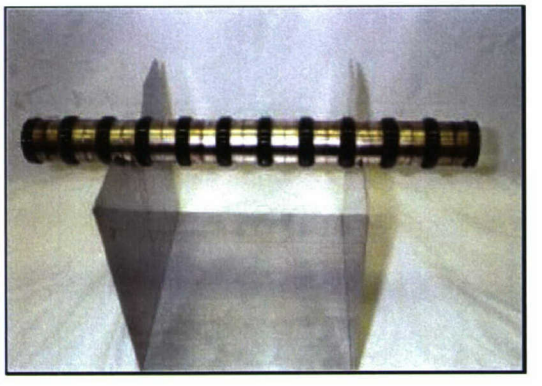

Fig. 2. 11-segment magnetic stack with ferrofluid rings.
This stack was used in the 3.1 second device.

If no ferrofluid is present, as a long magnetic stack moves inside a tube with a small gap between the magnet surface and the inside wall of the tube, a very slight deviation from the vertical position can cause the edge of the end of the magnet stack to touch the tube (Fig. 3). Due to the heavy mass of the magnet and large friction between bare magnet surface and the wall, this contact can impede or completely stop the oscillatory motion.

Fig. 4 shows the voltage output from a coil as a 1 kg mass, 20 cm long magnet stack was oscillating inside the tube. At the vertical orientation, with no contact between the magnet stack and the tube wall, the oscillations persisted for many cycles.

However, with the magnet stack inclined 4 degrees with a dry surface, the oscillations slowed down and stopped at one cycle after the tilting was applied. As the inclination angle increased to 10 degrees the oscillation ceased immediately. In another experiment, we placed Teflon discs on both ends of the magnet stack and applied 3-in-1 lubricating oil to the Teflon surface. The experiment was repeated under the same conditions. At 4-degree inclination, the oscillation slowed down and came to a complete stop after 2 and half cycles. The angle of inclination required to cause the oscillations to stop completely increased to 18 degrees from 10 degrees for the dry metal surface. However, after 24 hours of continuous oscillation at 2 Hz and 5-inch amplitude, the Teflon surface showed visible wear. Finally, with ferrofluid bearing as a lubricant, the situation improved drastically as the oscillation of the magnet stack sustained even at an inclination angle of beyond 45 degrees. Since the movement of a buoy in random ocean waves is a mixture of heave, pitch and roll that have velocity vectors in all directions, the unique property of the ferrofluid bearing enables the device to operate continuously.

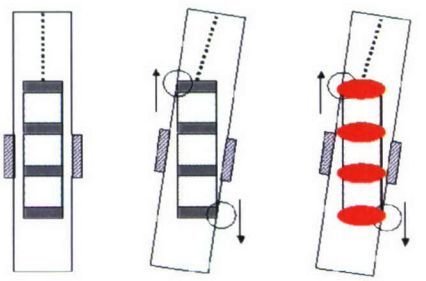

Fig. 3. Schematic of a magnet stake in a tube when it is vertical and tilted. The red area is the ferrofluid bearing, which prevents the magnet from making direct contact with the tube wall.

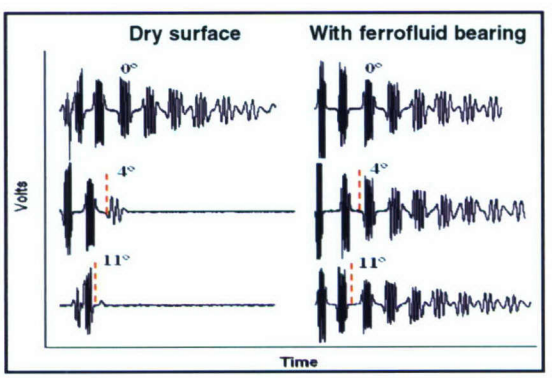

Fig. 4. Output voltage of the coil of a magnet stack with and without ferrofluid bearings. The tilt angles are 4 and 11 degrees introduced at a time marked by red dashed lines.

The most important design parameter of an axial type linear generator is the aspect ratio of each magnet segment. Since the induced voltage is proportional to the rate change of the magnetic flux density as the magnet stack moves through a coil, the maximum magnetic flux rate change is when the coil moves through the spacer between two magnets with opposite polarity.

This suggests the use of magnets with small aspect ratio in order to have the maximum number of magnet pairs and polarity changes within a given distance. However, as the aspect ratio decreases, magnetic flux starts to disperse and bend toward the side to return to the other surface. This fringe loss will reduce the net flux density. By calculating the flux density for various aspect ratios, we determined the optimum aspect ratio to be between 0.6 and 0.8 with the spacer's thickness about 15% of the magnet thickness. In the devices developed under this program, 1.2-inch long, 1.5-inch diameter magnets, and 0.2-inch thick low carbon steel spacers were used.

Finally, an axial linear generator is easy to fabricate and flexible enough to accommodate design changes. However, it also has disadvantages. For example, the device is limited to a straight-line configuration. A curved device would require custom shaped magnets with specific curvature. This configuration is costly and may affect the magnetic properties if the curvature is large. In addition, there is substantial amount of magnetic flux leakage. To prevent this leakage an axial design would require complex magnetic shielding. These shortcomings can be addressed by employing a transversal design.

3.3 Transversal linear generator

Fig. 5 shows the schematic of a transversal linear generator. In this design, the coils are shaped as thin disks and fitted into a cartridge between two rows of thin magnets mounted on low carbon steel yoke plates. Adjacent magnets on the same yoke plate have the opposite polarities and opposing magnets on different yoke plates have the same polarity. In this geometry, the combined flux from adjacent magnets flows through the coils, back into the yoke plates and finally returns through another coil to form a closed loop. In this configuration, the relative motion between the stator and the magnet stack is perpendicular to the flux lines through the coils. By using the commercial software for magnetic analysis, we calculated the total magnetic flux through a coil as a function of the gap dimension. If the gap is too large, the flux diminishes rapidly due to fringe field loss. In order to reduce the fringe field loss, the gap must be reduced. However, if the gap is too small, the flux density in the gap is high but the volume to accommodate induction coil is too small to be useful. We determined the optimum gap dimension between 0.2-inch and 0.3-inch. In this design, a very small amount of ferrofluid is applied to the region just between the coil and magnet surface to provide the near-zero-friction for the armature to slide over the stator cartridge. The transverse design is more difficult to make than the axial design. It has several advantages. The generator can be any shape including circular. In addition, the yoke plates serve as a magnetic shield to reduce the leakage. The principal disadvantage is the increased difficulty of fabrication.

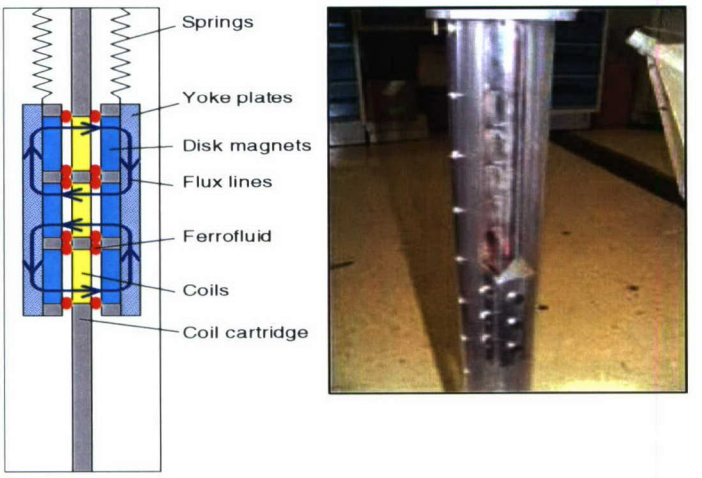

Fig. 5. Schematic and photo of transversal linear generator.

We fabricated one transversal linear generator unit to compare its performance with an axial linear generator of similar dimension. The sliding magnet/yoke plate assembly had 5 pairs of 1.5-inch x 1.5-inch area, 0.2-inch thick square magnets (NdFeB, N 42 grade). Output from 3 coils were combined and connected to a resistive load. The total weight of the moving magnet/yoke plate assembly weighed 0.6 kg. It was attached to a pair of Be-Cu springs to give the system a resonant period of 1.7 seconds. We measured its energy output by bench test under known excitation. The performance was compared to an axial configuration linear generator with the same spring-mass characteristics with comparable results. Therefore, there is no performance advantage inherent in this design. Since, for our geometries of interest, the axial design is much easier to make, it was used in all devices. For future devices where low magnetic leakage and curved shape are preferred, transversal design can be implemented seamlessly.

3.4 The mass-spring system of the linear generator

The linear generator in the wave energy harvester is configured as a mass-spring system. The mass consists of the magnet stack M_{mag}. It is attached vertically to a spring with a spring constant k. During operation, the assembly oscillates through a series of induction coils. In the absence of external damping, its natural period is $T=2\pi(M_{mag}/k)^{1/2}$. At the resonant frequency or the inverse of natural period, the oscillation exhibits a sharp peak with high amplitude. In practice, a resistive load such as a rechargeable battery and its associated electronic circuits is connected to the coil and it produces a counter electromagnetic force that will damp the oscillation. The damping lowers the amplitude and broadens the response peak.

Metal springs are adequate for most high frequency (< 2 second period) devices, because they require high stiffness and short extension. Springs made from non-magnetic materials are used in order to avoid the strong attraction by the magnet that can stop the oscillation. We have tried both phosphor bronze and beryllium-copper springs with good results. These materials are rated up to 2 million cycles. Longer lifetime can be achieved at reduced extension.

For low frequency operation (>2 sec period), the spring performance becomes more demanding. The required load, longer extension, and lower stiffness represent a set of specifications that metal springs have difficulty meeting. The brute force approach of using metal springs with extraordinary length is not practical. Very long springs can slow down the transmission of the torsion wave that travels from one end of the spring to the other end after a load is applied. The velocity determines the amount of energy that can be transferred via resonant coupling. A simple analysis shows that the ratio of the magnet stack mass to the spring mass must be greater than 40 for efficient resonant energy transfer to occur. Therefore, for low frequency device application, innovative solutions to fulfill the function of the spring are needed, as outlined in the following sections.

3.5 Magnetic spring

A pair of magnets placed with opposing polarity facing each other forms a simple spring due to the repulsive force. It is highly non-linear and has a very short range. A viable approach to extend the range and linearity is to stack a series of thin magnetic disks with alternating polarity. The magnets can be placed into a tube to keep them in line. This arrangement is equivalent to reducing the spring constant of traditional metal springs by connecting many units in series. The load versus displacement characteristics of such a magnetic spring made of ten 0.5-inch diameter, 0.1-inch thick NdFeB magnets is shown in Fig. 6. As expected, the useful range has been extended by adding more magnets. The elastic behavior is highly non-linear, but it can be viewed as a collection of piecewise linear segments for small displacements. This type of spring will be useful for a linear generator with high resonant frequency and small displacement.

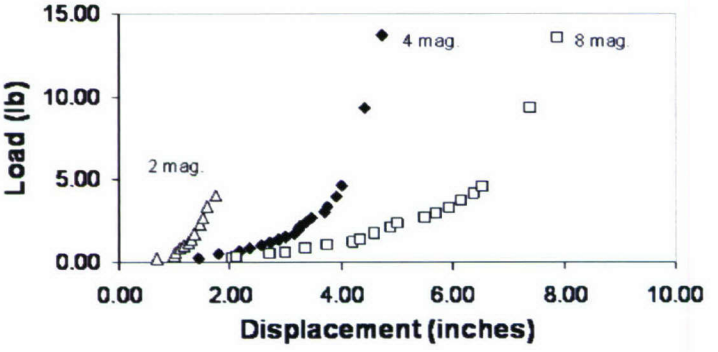

Fig. 6. Load and displacement relationship of a long-range magnetic spring.

3.6 Elastomer spring

The spring function can also be fulfilled by an elastomer hose or cord. Unlike metal springs, which are driven by torsion twist in the metal wire, elastomer springs are driven by molecular entropy. As elastomer is under a tensile load, the long-chain network opens up. After the load is removed, the elastomer will relax to the original state. We have tried different elastomer materials including Neoprene, Silicone, Buena, Viton and different types of latex. The best material is the virgin grade latex hose. Fig. 7 shows the elastic property of a 1/8-inch OD, 1/16-inch ID, 9-inch long latex hose and a metal spring with similar elastic properties.

The latex has a much higher load rating and is more stretchable than the metal spring. The latex spring elastic property is slightly non-linear, but this effect is not significant enough to be detrimental to device performance. The extremely light weight of the latex makes energy transfer from one end to the other very fast and energy coupling more efficient. These properties were verified by bench test. We have used latex hose in the large devices with 2-3 kg magnet stacks used in the 2.1-sec and 3.3-sec devices.

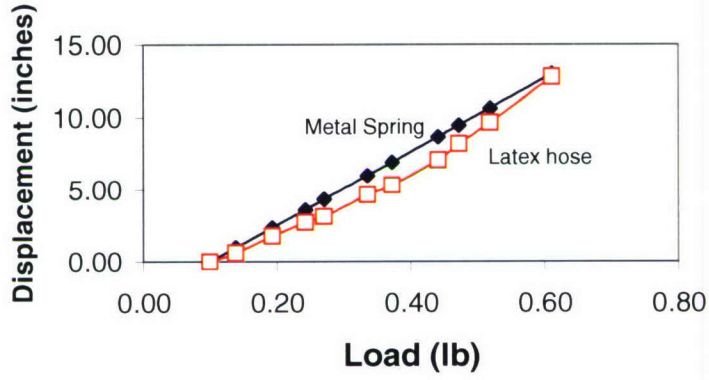

Fig. 7. Elastic properties of a virgin grade latex hose.

Despite these attractive advantages, latex hose spring has one serious drawback that is common to all elastomers – the continuous sagging under load. Sagging is an irreversible process and can shift the equilibrium position of a mass-spring system slowly with time. The major cause is believed to be due to the oxidation of sites that are exposed to air during stretch, preventing the elastomer chains from returning to their configuration. Further studies will be necessary to thoroughly understand the cause and find solutions to make the use of latex spring a practical alternative to metal springs.

3.7 Linear generator characterization

Bench tests were carried out to accurately determine the linear generator characteristics including the energy capture rate and energy conversion efficiency. In the simple set up, a mass-spring type linear generator was attached to the end of an excitation spring with a spring constant k_{ex}. The linear generator described in this measurement had a two segment magnet stack. Each segment contained a cylindrical Grade 42 NdFeB magnet (0.5-inch diameter and 0.375-inch long), with 0.125-inch thick soft iron disk spacers placed between the two magnets and on both ends as caps. The magnet stack was connected to a spring giving the system a resonant frequency of 0.82 Hz. Two induction coils were wound on the tube to match the spacing of the magnet stacks. Each induction coil consisted of 700 turns of size 32 wires. Their outputs were connected in series but with reversed polarity to combine the total energy. The output was connected to a load resistor with the same resistance as the coils. The linear generator was then stretched by extending the excitation spring to an initial displacement of ΔL and then releasing the spring. The energy stored in the stretched excitation spring was coupled into the linear generator and its output voltage was recorded on an oscilloscope.

When the coil was an open circuit, there was no damping caused by counter EM force. It took more than five minutes for the oscillation to reach half value of its initial amplitude. This indicates that the energy loss due to air resistance and internal loss of the spring is negligibly small. After a resistive load was connected to the output, both the oscillations of the magnet stack and the linear generator attached to the excitation spring came to a near stop within seconds after the stretched excitation spring was released, a signal that the system was critically damped. The excitation energy was transferred to the linear generator and converted to electrical energy. The total input energy was calculated from the spring formula $E=0.5*k_{ex}*\Delta L^2$. The amount of energy converted to electricity after each passing of the magnet stack through the coil was calculated from measuring the voltage output across the load with an oscilloscope. The dependence of energy output after pulsed excitation is shown in Fig. 8.

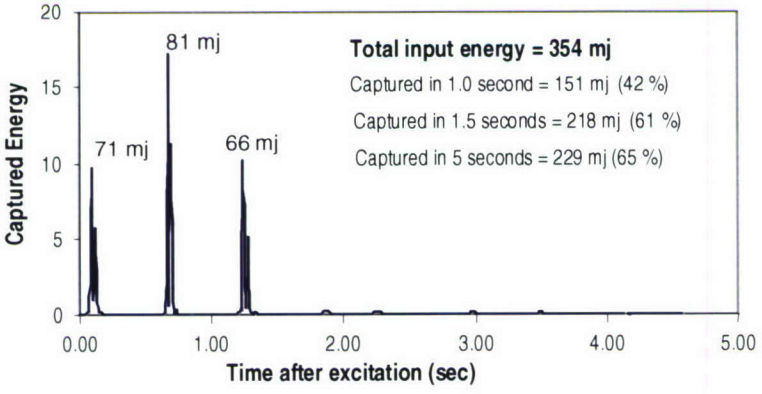

Fig. 8. Single pulsed excitation bench test.

In the example shown in Fig. 8, the input energy was 341 millijoules (mj) which was transferred rapidly to the linear generator. After 1.5 cycles, 218 mj of energy was converted to electrical energy, representing an efficiency of 61%. Most of the remaining energy was dissipated as heat in the coils. Total energy lost in the spring was less than 3%. We repeated the experiment by stretching the excitation spring to different initial displacement lengths and also on devices with heavier magnet stacks and more coils. Similar results were obtained in all cases with conversion efficiency between 55-65% after 1.5 cycles of oscillation. **In summary, the simple mass-spring type linear generator with optimized magnet stack design and near zero friction ferrofluid bearing has high conversion efficiency and fast energy capturing process at low operating frequency. It is an ideal power take off device for wave energy harvesting devices.**

3.8 Computer simulation for pulsed excitation

The efficiency measurement by using a pulsed mechanical energy excitation source can be modeled by computer simulation. We developed this software by solving a set of coupled equations of motion: one for the movement of the magnet stack of the linear generator and the other for the movement of the linear generator housing and the excitation spring. Initial conditions were chosen to describe the pulsed excitation caused by releasing the stretched excitation spring.

In this model, the input parameters are the linear generator's mass spring characteristics, the excitation spring constant, its initial displacement, and finally the mass of the linear generator housing. The first equation also includes a damping term to represent interaction between the moving magnet and the induction coil when it is connected to a load. The damping coefficient was determined in a separate series of experiments. The simulated temporal evolution of the amount of energy captured by the coils is shown in Fig. 9. These data show that over 90% of the total harvested energy was captured in the first 2 seconds. The rapid energy capturing process is in excellent agreement with the measurements.

With the model validated in this simple case, the model was later refined to include a periodic excitation forcing function. That refined model was used to simulate performance of a buoy-based wave energy harvesting device in response to single frequency sinusoidal waves, as described in detail in Section 5.

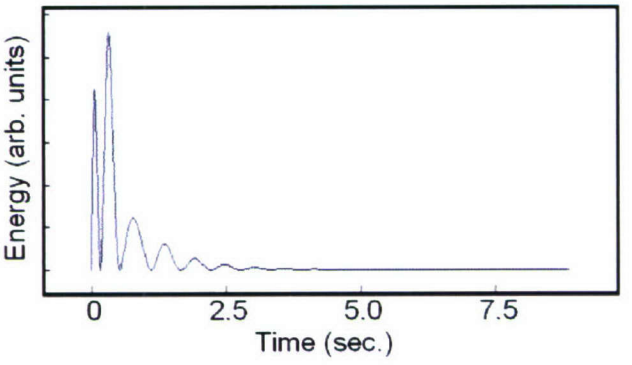

Fig. 9. Results of model simulation confirms fast energy capture and high efficiency.

4.0 Spar buoy hydrodynamics and wave tank testing

After the development of the linear generator (Section 3), the next step was to develop a platform that can couple with the wave motion and efficiently transfer energy to the generator. One approach is to integrate the linear generator to a spar buoy. "Spar buoy" is a general term used to describe buoys with a long and slender body. Because of the hydrodynamic properties of a spar buoy, its interaction with waves is strongly dependent on the length submersed in water (known as the "draft"). Spar buoys with very long draft are often used to stabilize floating platforms because their very long natural period causes them to act as a mechanical filter that isolates itself from slower movements. A spar buoy can also be made extremely unstable if the natural heave period is tuned to the most probably wave period at the deployment site. Under this circumstance, its heave movement will be enhanced to be several times higher than the waves. This property can be applied to wave energy harvesting by using the spar buoy as a platform for the wave energy harvester. This concept was studied in great detail by hydrodynamic analysis and well controlled wave tank tests at The University of Rhode Island Department of Ocean Engineering headed by Prof. Malcolm Spaulding and Stefan Grilli.

The collaborative study covered extensive theoretical modeling to optimize the heave enhancement of spar buoys and to reduce its pitch and roll motion. Finally, a scaled down energy harvester was tested in the URI wave tank with and without linear generator. A detailed description can be found in the attached URI final report.

5.0 Linear generator on a spar buoy platform

In parallel with URI's theoretical and wave tank studies on spar buoys, TSC carried out numerous laboratory bench tests and computer simulations on a full-scale model of this design. Although both bench tests and simulation models were based on a single frequency sinusoidal forcing function instead of the random motion of ocean waves, the results did provide much valuable information and insight. Results serve as guidelines for device design such as the dimensions and required specification of various components. The simulation studies also revealed surprising features such as frequency broadening by varying the electrical load and the existence of a double peak response in the power vs. wave period dependence. Finally, from the model simulation and bench tests, we proposed an adaptive approach involving a sensor-controlled load switching mechanism to maximize power output over a wide range of wave conditions.

5.1 Computer model simulation

The computer model used to determine the response of a mass-spring type linear generator under pulsed stimulation (Section 3.8) was modified by replacing the pulse excitation forcing with a sinusoidal forcing to represent the waves. A second oscillator was also added to simulate the spar buoy. The two oscillators are closely coupled. Detailed formulation of the model is described in the following sections.

5.2 Defining the intrinsic frequency of a buoy

The oscillator characteristics of a spar buoy can be understood by considering the following case. A cylindrical shaped buoy with a base area A and draft (submerged length) L acts like a linear spring. When load F is applied to the buoy, it will push the buoy into the water by a displacement ΔX such that the applied force equals the added buoyancy or:

$$F_{load}=\rho A\Delta X$$

where ρ is the density of the water. When we compare this expression with the spring formula $F=k\Delta X$, it is obvious that the buoy can be regarded as a linear spring with a spring constant

$$k_{buoy}=\rho*A$$

The natural heave period of the buoy is determined from:

$$T_{spar}=2*\pi*\left(M_{buoy}/k_{buoy}\right)^{1/2}$$

Since the buoyancy force equals to the gravitational force of the buoy mass or:

$$M_{buoy}*g==\rho*A*L$$

Substituting these equations yields the expression of the natural period as:

$$T_{spar}=2*\pi*(L/g)^{1/2}$$

This is the basic formula for spar buoys and is independent of the buoy diameter.

Once we have determined the oscillating characteristics of the buoy, we can create a set of coupled equations of motion for the following system shown in Fig.10.

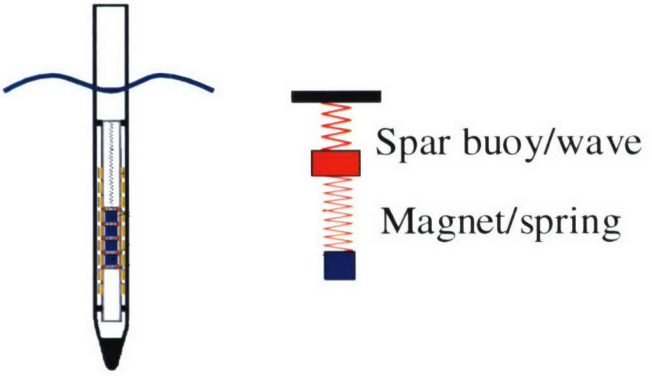

Fig. 10. Schematic of a laboratory representation of a spar buoy based wave energy harvesting device in waves.

5.3 Input parameters

Input parameters used for this simulation mode are:

1. m_1: Buoy mass, including the housing and coils of the linear generator that are mounted onto the buoy, but not including the oscillating mass and spring inside it.
2. h_0: Buoy draft at equilibrium
3. Wave condition: We assume single frequency sinusoidal wave as the water level Δh varies as $\Delta h=A\sin(2\pi t/T)$, where A is the wave amplitude (one half of the wave height and T is the wave period).
4. γ_1: The friction coefficients between water and the buoy (i.e. drag), given by $-\gamma_1(\frac{dy_1}{dt}-\frac{d\Delta h}{dt})$.
5. m_2: The oscillating mass of the linear generator
6. k_2: The elastic constant of the linear generator mass-spring system.

7. γ_{12}: The friction coefficients between the weight and the buoy (i.e. the interaction between the moving magnet with the counter EM force produced by the coil when the output is connected to a resistive load). The force is $-\gamma_{12}(\frac{dy_1}{dt} - \frac{dy_2}{dt})$

We set up the two equations of motion as follows:

$$k_1(\Delta h - y_1) - k_2(y_1 - y_2) - \gamma_{12}(\frac{dy_1}{dt} - \frac{dy_2}{dt}) - \gamma_1(\frac{dy_1}{dt} - \frac{d\Delta h}{dt}) = m_1 \frac{d^2 y_1}{dt^2}$$

$$k_2(y_1 - y_2) + \gamma_{12}(\frac{dy_1}{dt} - \frac{dy_2}{dt}) = m_2 \frac{d^2 y_2}{dt^2}$$

The first equation represents the buoy movement, and the second equation represents the motion of the oscillating magnet stack inside the linear generator.

5.4 Simulation results

Results from the simulation give us the following information:

- Output power (Watts)
- The displacement of magnet from its equilibrium position as a function of time. This quantity is strongly dependent on the resistive load across the coil output. It can be used in device design to keep the spring displacement within its specified extension limit.
- Heave height and phase of the buoy as a function of time. This is strongly dependent on the drag coefficient of the buoy. If a very high drag coefficient is chosen, the buoy will act like a wave rider. This can be used in buoy design to control the heave motion.
- Phase difference between the magnet oscillation and the buoy heave movement. This is an important quantity, and depends on the difference between natural frequencies of the linear generator and the buoy.

Fig. 11a and 11b show a graphic output of the simulation results for two cases. In this example, the wave period matches the natural period of the buoy at 2 seconds or 0.5 Hz, but differs from the natural frequency of the linear mass-spring generator.

The top half of each graph shows the oscillation amplitude and phase of the buoy (in blue color) and the magnet stack (in brown) with respect to the water surface at rest. Constant wave motion (in green color) is also displayed as a reference. The lower half of the figure shows the net displacement of the magnet stack from its equilibrium position. This can be obtained from the difference between the position of the magnet stack and the buoy at any instant, since the coils are secured to and move with the buoy. Results are highly dependent on the relative natural period of the buoy and the mass-spring system of the generator. Figure 11a shows a case in which the linear generator's natural period (1.26 second) is shorter than the buoy (2 seconds), their oscillations are in phase but with different amplitude. Figure 11b shows a case in which the natural period of the linear generator (2.8 second) is longer than the buoy.

Their oscillations are out of phase but with similar amplitude. Because the oscillations are out of phase, the net displacement of the magnet from its equilibrium position is actually greater, producing more power.

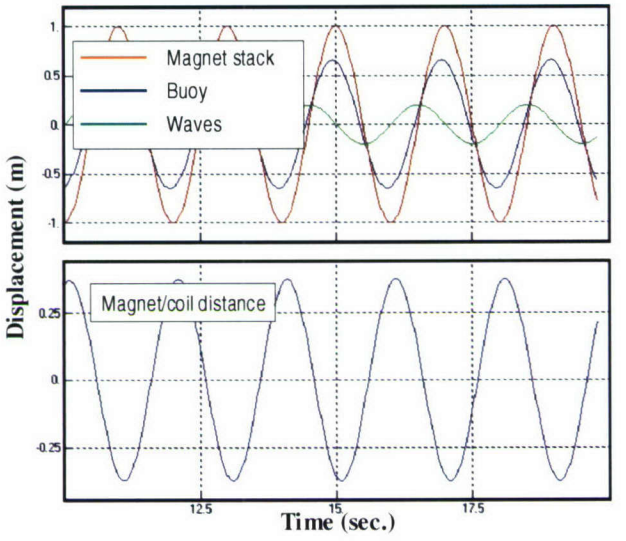

Buoy	
Draft (m)	1
Mass (kg)	20
Period (s)	2
Generator	
Spring (N/M)	50
Mass (kg)	2
Period (s)	1.26
Waves	
Height (m)	0.4
Period (s)	2
Gamma	
γ_1 (N-m/s)	5
γ_{12} (N-m/s)	20
Power (W)	2.4

Fig. 11a. Simulation results (case 1): Generator has shorter natural period than the buoy.

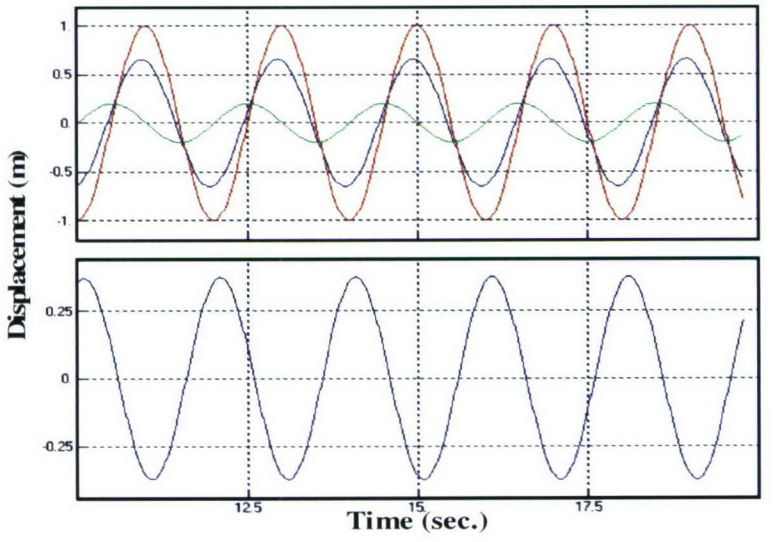

Buoy	
Draft (m)	1
Mass (kg)	20
Period (s)	2
Generator	
Spring (N/M)	50
Mass (kg)	2
Period (s)	1.26
Waves	
Height (m)	0.4
Period (s)	2
Gamma	
γ_1 (N-m/s)	5
γ_{12} (N-m/s)	20
Power (W)	2.4

Fig. 11b. Simulation results (case 2): Generator has longer natural period than the buoy.

Other unique properties of the spar buoy based wave energy harvester:

Several unique properties are demonstrated by the spar buoy-based wave energy harvester, as follows.

Power output is dependent on spar buoy mass. Because a mass-spring type linear generator and frequency matched spar buoy form a pair of coupled oscillators, the two individual vibrational modes become degenerate to form two normal modes at different frequencies. The spar buoy is not only a platform but an active part of the working device. In operation, it acts as an energy reservoir that is continuously replenished by taking energy from the waves. At the same time, it transfers energy to the linear generator for conversion to electricity. This simple mechanism allows the system to effectively couple in energy from the ocean wave in a hermetically sealed structure. The spar buoy mass also plays a role in energy harvesting as a part of the "reduced mass" of the system. Therefore, a spar buoy based wave energy harvester can produce a large amount of energy without using very large magnets. The advantage is offset by the need for springs with extremely demanding performance specifications.

Multiple peak response and adaptive switching are demonstrated. In any linear coupled oscillator system, such as the spar buoy mounted linear generator, there are two normal vibrational modes: a symmetric and an asymmetric mode. In the symmetric mode, the spar buoy heave and the linear generator magnet oscillation are out of phase, either moving away or moving toward each other. In the asymmetric mode, the spar buoy and the magnet stack always move in the same direction but with different amplitude. The position and width of the two peaks depend on the electrical load, as shown in Fig. 12. With a large load, the two peaks are sharp with large peak value, characteristics not suitable for wave energy harvesting. As the load decreases, the damping due to counter EM force interaction increases and broadens the peaks to cause them to merge. As a result, the output power vs. wave period curve shows a broadband response that is beneficial to wave energy harvesting. Further decreasing the load will merge the two peaks to form a single peak. This interesting load dependent response suggests an "adaptive switching" approach to further broaden the harvester response in time varying random ocean waves. Its operation can be seen in Fig. 13. The approach is to install an on-board accelerometer to monitor the wave period. When it senses a change at one of the two set points (S1and S2), determined by the intersection between the low load single peak response and the high electrical load double peak responses, the electrical load will be switched between low and high loads. Therefore, the overall response curve will follow the higher value of the two response curves to cover a very broach range of wave conditions. The "adaptive switching" scheme consumes a very small amount of power but can improve the device significantly.

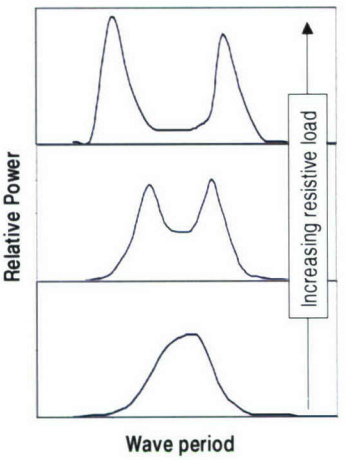

Fig. 12. Power output versus wave period curve for different loads, illustrating the qualitative differences in spectral response.

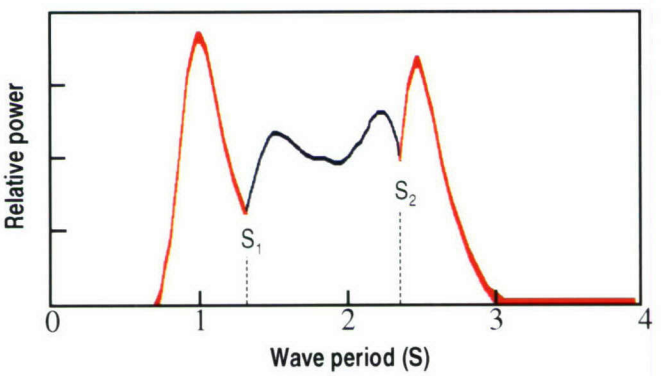

Fig. 13. The schematic of "adaptive switching" to broaden device response.

5.5 Bench tests

A simple laboratory test bench was set up to characterize the wave energy harvester performance and to validate the simulation model accuracy under single frequency sinusoidal wave excitation. Fig. 14 shows a picture of the bench test set up. A steel cable is looped around a pulley mounted on the ceiling. One end of the cable is attached to the rotating arm driven by a variable speed DC motor. The distance between the off-center point where the cable is attached to and the center of rotation determines the "wave" amplitude (i.e. half wave height). The other end of the cable coming down from the pulley is connected to a large spring ("buoy spring") to mimic the buoy movement. A linear generator tube containing coils and mass-spring magnet stack is attached to the end of the buoy spring. As the DC motor rotates, the cable moves in the vertical direction by a total displacement of twice the distance of the "wave amplitude". This movement drives the first oscillator consisting of the linear generator (not including the mass-spring system), or the "buoy". The movement of the buoy spring is coupled to move the magnet stack-spring system inside the linear generator housing.

Because of the limitation in ceiling height, we carried out all measurement by setting wave heights to 0.14 meters and wave periods from 0.8 sec to 4 sec. Power output from different resistive loads were measured.

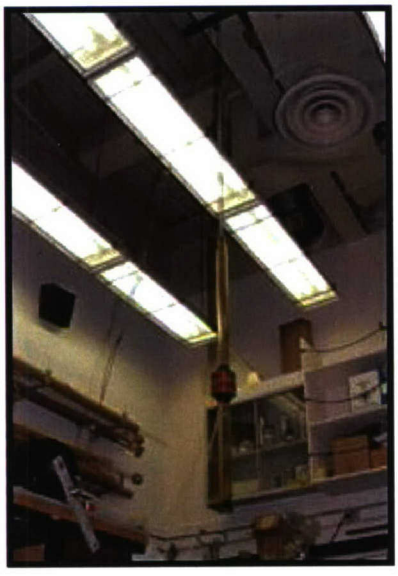

Fig. 14. Bench-scale laboratory test set up for simulating single-frequency "dry wave tank" experiments via a pulley and motor drive system.

Each linear generator was measured in two settings. In the first setting, the linear generator was directly attached to the cable without the buoy spring. This was used to simulate the case where the buoy was a wave follower. In the other setting, a buoy spring was used and the two oscillators were tuned to the same frequency. This set up simulated the effect of a wave energy harvester with a tuned spar buoy as the platform. Among four devices with various magnet size and springs, excellent agreement was found between the measurement and calculation results in all cases. An example is given for the test results of a linear generator with a 3 segment magnet stack with a total mass of 1.03 kg and two induction coils connected in series with a total resistance of 7.2 ohms. The natural period of the linear generator is 1.46 sec. Extensive measurements were made from 2.2 sec to 0.8 second under various conditions. Results are shown in Fig. 15 and Fig. 16.

Fig. 15 shows the power output of the device mounted directly to the cable without the buoy spring. Measurements were made for three different load resistors. As the electrical load resistance increased, the damping due to the counter EM force decreased and a peak at the natural period of the generator emerged. In all cases, the measured and calculated results are in excellent agreement. In this set up, the buoy acts as a wave follower and the power output is independent of the buoy mass. The only way to increase the power output is to increase the weight of the oscillating mass in the linear generator. This corresponds to either a heavier magnet stack or a non-magnetic ballast added onto the magnet stack.

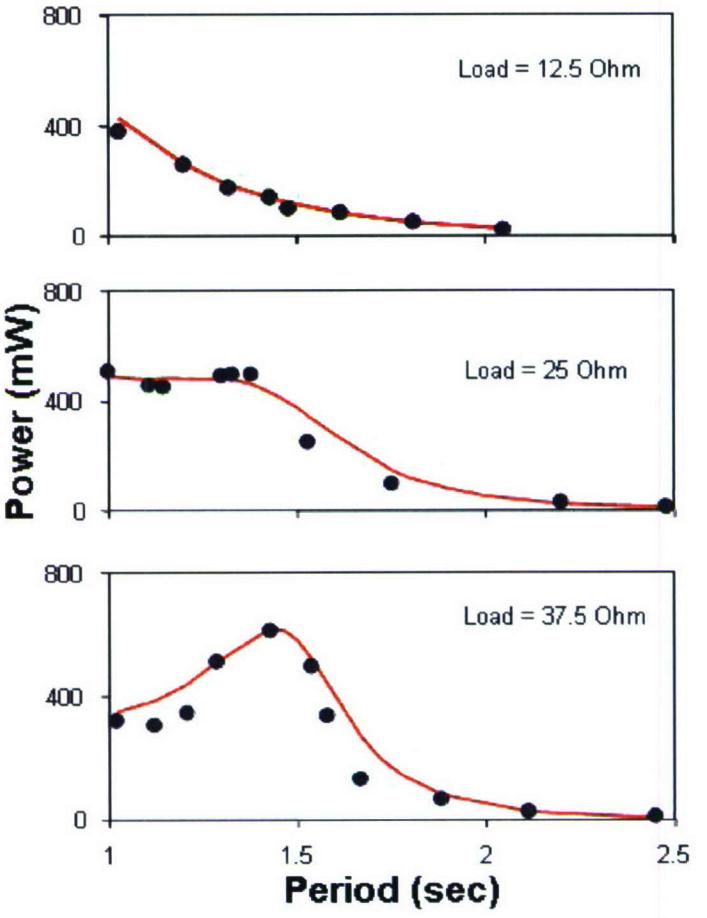

Fig. 15. Bench test and model simulation results of an energy harvester on a "wave follower" buoy.

Fig. 16 shows the power output from a similar device (1.0 kg magnet stack, 1.43 sec. natural period) but mounted to a "buoy spring" to mimic a spar buoy based device. The natural period of the "buoy" is tuned to 1.63 sec. and the weight is 2.8 kg. Two sets of measurements were made. In one set, each coil was connect to its own load and measured separately. The total power output was taken as their sum. In another measurement, power output from each coil was combined by a rectified bridge. The combined output was measured. The agreement between the measurements and the model calculation were again excellent. The response spectrum of the two-oscillator device differs from the one oscillator device considerably. With a large electrical load of 50 ohms, the power output in the wave period range from 1-2 seconds has a double peak response corresponding to the two normal modes of the coupled oscillator. As the electrical load was reduced to 25 ohms, increased damping forced the two peaks to merge into a single peak with higher peak value.

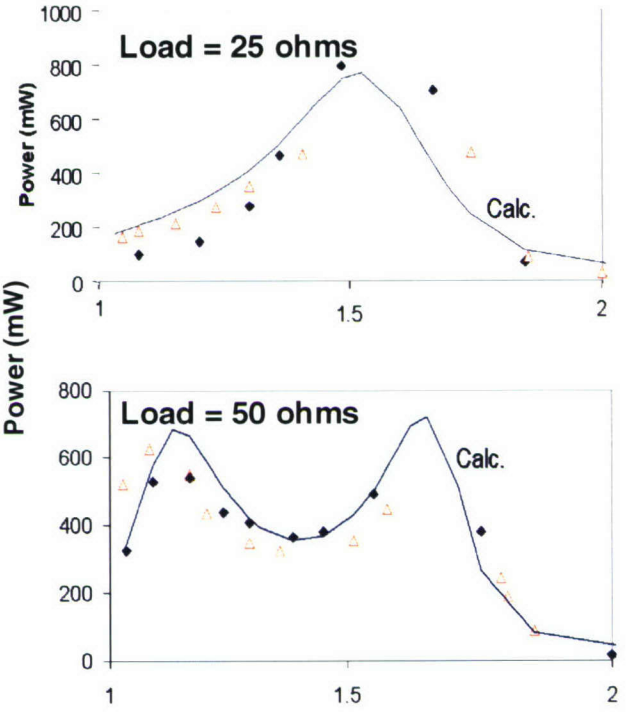

Fig. 16. Bench test and model simulation results of an energy harvester on a simulated "spar buoy".

Finally, we should point out that despite the good agreements between the bench test and model calculation, these results predict the performance under single frequency, sinusoidal forcing functions. Ocean waves are random in amplitude, phase, and direction. Their effect on the device performance will be the sum of all Fourier components. Further tests subject to a random forcing are needed. The simulation model also needs to be expanded accordingly to include a more realistic scenario.

6.0 Full-scale spar buoy device fabrication and field test

This task was performed in collaboration with Oceanscience Group, a manufacturer specializing in fabrication of buoys and floating instrumentation platforms. Three devices were made and a total of five tests were carried out in Oceanside harbor.

Among the three devices made, the first two were single spar buoys for long period wave operation. The third device, named "tetra-buoy", consists of 4 small spar buoys connected by a bracket. It is specifically designed for operation in waves with periods of ~1. 5 second.

6.1 2.3-Second device

This buoy was made from 6" diameter vinyl pipe with a low drag nose cone at the bottom (Fig. 17). External lead ballast was added to the tip of the cone to increase stability so the spar buoy could stay floating vertically in water unattended (Fig. 18). The submerged length was 1.45 m and it had a natural period with the linear generator disconnected of 2.3 sec. The total weight including the linear generator was 22 kg. The linear generator had 8 segments of 1.5" diameter, 1.2" tall cylindrical magnets (NdFeB Grade N42) with 0.25" thick low carbon steel spacers. The total weight was 2.62 kg. We used four strands of 1/8" OD, 1/16" ID virgin grade latex hose as springs. These elastomer springs were pre-sagged under a static load of 3 kg for 48 hours in order to slow down the sagging process. A total of 4 induction coils were used. Two of them were around the equilibrium position. The other two coils were placed at 12" from the bottom to slow down the magnet stack and prevent it from hitting the bottom. The outputs from all coils were connected to 15 ohm loads and the data was stored in the memory card of an on-board data logger. The output from each coil was summed to obtain the total power output.

Fig. 17. 2.3-second spar and matching linear generator

Fig. 18. 2.3-second spar and linear generator device in the water

6.2 3.1-Second device

This device was similar to the 2.3-second device except for a much longer draft in order to have the longer natural period. The 11-segment magnet stack had a total mass of 3.2 kg (Fig. 19). Again, we used latex hose as the spring to handle the heavy mass. The buoy was made from 4.5" diameter vinyl pipe with a low drag nose cone at the bottom. Its total mass including the linear generator was 23 kg. It was 3.2 meters long with 2.5 meter submerged under water to achieve a natural period of 3.1sec. Because of its extreme length and small diameter, this buoy could not stay vertical in water. When it interacted with waves, in addition to heave there were a lot of pitch and roll movements. These parasitic movements were a probable energy drain.

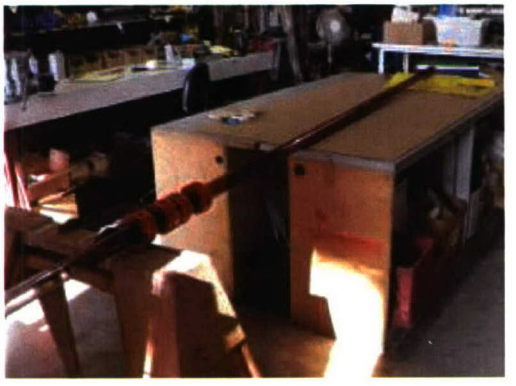

Fig. 19. Linear generator for the 3.3 second device (spar not shown).

6.3 Field testing

A total of four tests were carried out for the single spar buoy devices at the Oceanside harbor, two tests for each device. The devices were driven by the wakes from passing ships. We were able to find waves (3 sec. 10" and 2.4 sec. 10") that were closely matched to the natural period of the devices. **However, we should emphasize that this kind of "artificial" wave is very different from the ocean waves in many ways. They were unidirectional and sinusoidal with only a single frequency. In addition, their period and wave height relationship does not follow those in the wind wave power spectrum for various sea states.** For example, the 3.1 sec period waves found between Sea State 2-3 should have a significant wave height between 30"-40" instead of 10" high wakes. More controlled tests in real ocean environments with measured waves and winds are clearly needed, and the lack thereof represents a deficiency of the current effort.

Fig. 20 and 21 show "in the water" results for the 2.3-second device and 3.1-second device, respectively. The 2.4 sec. device produced over 6 Watts of power, and the 3.1 sec. device produced only 4.1 Watts. We attribute this discrepancy to the fact that the waves used during test were boat wakes that have much lower wave height than wind waves with the same period.

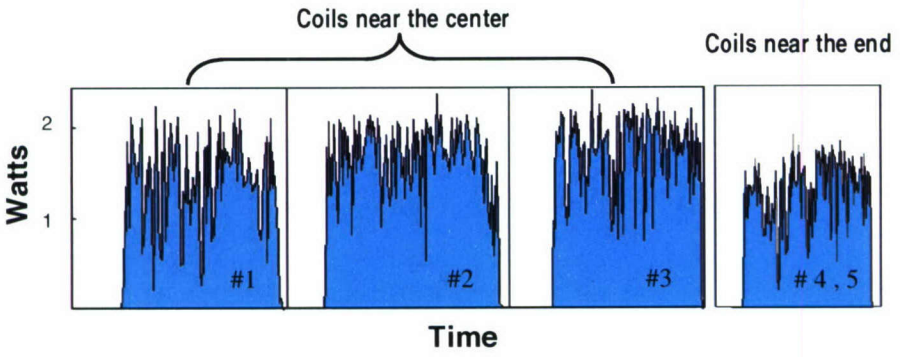

Fig. 20. Field test results of the 2.3 second device.

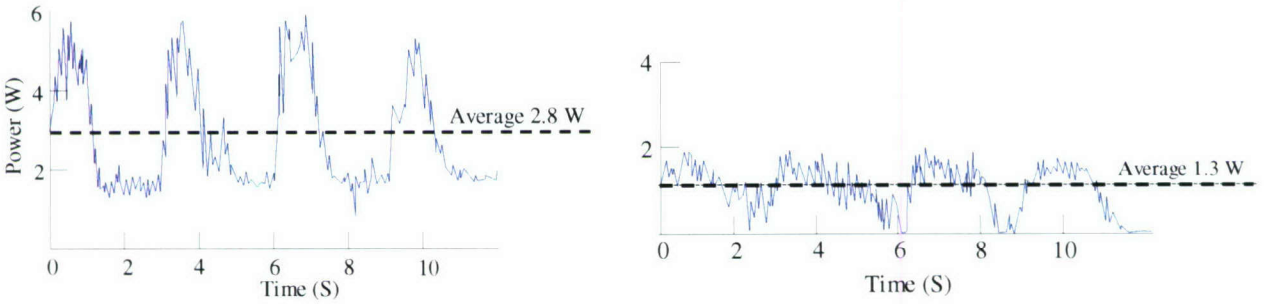

Fig. 21. Field test results of the 3.1 second device

6.4 Tetra-spar buoy device

The best window in the wave spectrum to operate a spar buoy based wave energy harvester is for wave periods below 2 seconds. For longer wave period, the spar buoy must be extremely long. With longer devices, hydrodynamic instability and spring performance become issues. For operation in shorter wave periods, the spar buoy must have short draft such that the center of mass and center of buoyancy are too close to each other. This makes the system unstable, and also lacks sufficient buoyancy to have any load. Based on the studies by URI, one solution was to form an array of short spar buoys to increase its footprint, buoyancy and stability while maintaining its heave characteristics in fast waves. We took this approach and built a tetra-spar unit shown in Fig. 23. The center spar contained a 1.48 sec period linear generator. Three equally spaced satellite spars were connected to an above surface bracket to provide stability and buoyancy. The unit weighed 21 kg and had natural period of 1.75 sec that was considerably longer that the on board linear generator. The device heaved with the small wind waves in the harbor and produced 1.6 Watts of power.

Fig. 22. A tetra-spar buoy wave energy-harvesting device.

7.0 Underwater energy harvester

Task 3 of the program was to develop a small energy harvester for under water operation. The device was to be mounted to a dogfish to harvest energy from its motion. Due to the small fish size (approximate 40-50 inches, 25 pounds), the device was targeted to weigh no more than 0.2 kg, and needed to produce 200 mW of power when the fish is swimming. Dogfish belong to the shark family. Dogfish are slow swimmers, spending most of the time near the bottom. This type of fish has a long tail, which moves at about 1.7 sec per cycle with amplitude of less than 10 inches.

Two types of devices were built and tested. The first device was a rotary generator, of which we tested two different designs. The second device was a translation generator with an oscillating magnet stack on ferrofluid bearings in a tube between two recoil end magnets. Output power was extracted by coils around the tube. Device of different designs and size were tested in a swimming pool under different motion parameters.

7.1 Rotary generators

We tested two types of rotary devices. One device had low magnetic flux density through the coils and must be operated at high rotational speed. The other device had high magnetic flux density through the coils and can be operated at low speed.

In the first device, we removed a small rotary generator from a commercial hand-cranked flashlight. This generator was only 1.5" diameter by 1" tall. The area of the magnetic field was small, so its performance must be compensated by operating at high rotation speed. Therefore, we modified the device by connecting the rotor shaft to a small 11:1 up-conversion gearbox. The driving shaft of the gearbox was connected to a 5" long rod with a 3" diameter impeller plate at the end. A spring-loaded Teflon O-ring seal was installed around the shaft to keep the inside of the device dry.

We drove the device by pushing the impeller through water back and forth with 10" amplitude at 0.5 m/sec to mimic the tail movement of the dogfish. However, the output power was only 2 mW, which was orders of magnitude lower than the target performance.

The second rotary generator was custom built to give very high magnetic field density through the coils for slow speed operation. A picture of this device is shown in Fig. 23. It had a transversal design (Section 3.3) with a total of eleven pairs of 0.75" diameter, 0.1" thick NdFeB magnet disks and a equal number of coils. Because of the extensive use of magnets and yoke plates, the device was very heavy at 0.4 kg. During operation, the magnets and yoke plates were stationary, with the coils moving in the gap between the magnets. The shaft was connected to a rod and a 3' diameter impeller. When the impeller moves back and forth in water, it drove the coils through the magnetic gap to produce power. At 0.5 m/sec velocity and 10" amplitude, this device could produce 6.5 mW. Although a slight improvement, power output was still far below the target performance (200 mW).

Fig. 23. An exposed view of the two halves of a rotary generator with high magnetic flux for under water application. Flat disc coils and magnets with alternating polarity are marked + and – The assembled rotary generator is shown in the lower right corner.

7.2 Translational generators

Because the rotary generator failed to approach the power requirement goal within the limit of device size and operational conditions, we also tried a linear generator design. We carried out detailed measurements and established complete metrics to assess its feasibility.

The device was hermetically sealed and designed to operate from a horizontal position such as mounting on the tail of a dogfish. Its simple structure consists of a magnet stack sliding reciprocally on ferrofluid bearings inside a tube through a set of coils. A pair of recoil magnets was mounted at the end of the tube to assist the oscillatory motion shown in Fig. 24.

Fig. 24. A linear device for underwater operation.

We made three devices with mass of 0.2 kg, 0.4 kg and 0.8 kg. They were excited by oscillatory sideways movement with a full amplitude of 0.2m, 0.3m and 0.4m, respectively. Each measurement was repeated for three different oscillatory periods at 1.0 sec., 1.3 sec., and 1.7 sec. The performance metrics are shown in Fig. 25. Just as the rotary generators, the translational generator also failed to meet the target performance

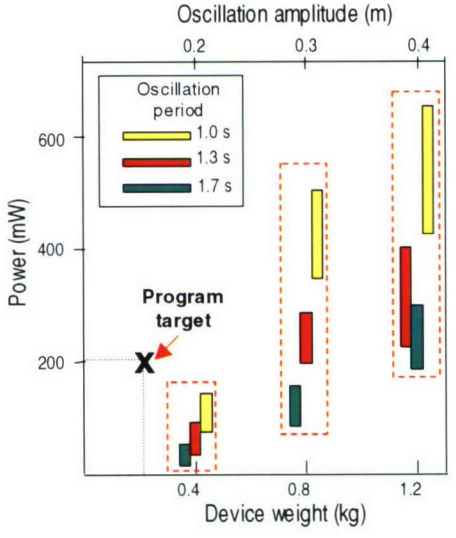

Fig. 25. A translation underwater device performance.

Based on this extensive study, we concluded that within the imposed restrictions in device size and movement, it is not possible to deliver the 200 mW of power required by the target performance. We therefore, in consultation with the DARPA program manager (E. Carapezza) did not pursue this design further.

8.0 Implications for further research

Our studies on spar buoy based wave energy harvester point out many unique advantages of this technology. But at the same time, they also reveal its limitations. Key limitations include:

(1) The natural period of the spar buoy must be tuned to match the wave condition at the deployment site for best performance. Therefore, the design becomes time and site specific. Oceans wave are random and vary with time.
(2) Spar buoy device for very low frequency operation in high sea states demands extremely high performance springs, which are beyond the state of current technology.
(3) The required length of the spar buoy is proportional to the square of the wave period. As the wave period increases with sea state, the spar buoy can become too long to be practical. For example, a spar buoy to harvest energy from the 10 second waves will be more than 25 meters long.

Further research is needed to address these problems. The two major areas are described in the following:

To develop a realistic simulation model: The computer model developed under this program deals with single frequency, sinusoidal driving force. The actual device performance could be vastly different in random ocean waves. A more realistic model must be developed to accurately use the forcing function based on wave data to include the effect due to random waves and currents. The model must be validated by field tests in real waves. Only then could the model be used for a realistic trade study to design optimally effective buoy-generator systems.

To broaden the device response over a wide range of sea states: Our approach has largely been focused on harvesting energy from the most significant waves at a given sea state. Therefore it is site and time specific. However, the most significant wave only represents a small slice in a broad wave spectrum that contains a continuous distribution of different wave periods. Since marine instrumentation generally requires 1-50 watts of power, it is no longer necessary to tune the buoy to the most significant waves. For example, we can design a device for the smaller but faster waves. These waves are ever present in all sea states. This represents an additional design option, for specific cases, that was not pursued in this Phase 2 program.

9.0 Conclusions

Harvesting energy in the range of 1-50 Watts from ocean waves in moderate sea states is very promising using the Wave Energy Harvesting device design created by TSC. The nearly frictionless ferrofluid-based mass-spring power generator design is robust and efficient. When properly coupled to a "buoy platform", this technology has the potential to generate tens of Watts of power on a continuous basis.

The numerical model created during this program was helpful in the initial buoy design. However, in order to provide accurate predictions of the wave energy harvester power generation capability in given sea conditions the effects of random waves, ocean currents, and local wind fields must be added to the model.

Axial generators should be used for all systems which allow for a linear design. Axial generators are more easily produced and provide comparable power when compared with transversal generators. Transversal generators can be employed for designs which require curvature, though they are difficult to produce, and require spring performance which is not easily achieved.

Extensive research and testing on springs was conducted during this program. Phosphor-bronze and beryllium copper springs were identified as acceptable solutions for devices tuned to high frequency waves with periods less than 2 seconds. Elastomer springs were identified as acceptable for devices tuned to lower frequency waves, although sagging could potentially become a major issue over the life of the device.

The wave power generator was tested extensively and proven to have a very efficient power take off design which regularly captures 55-65% of the available wave energy within 1.5 cycles.

Techniques to adaptively change the load on the wave energy harvester have promise to improve the total power generation and should be explored in more detail and field tested.

The attempt of designing a device which meets the requirements for mounting on dogfish and generating 200 mW of power was not successful, and we recommend abandoning this approach.